

decay with a lifetime less than 10^{-11} seconds, too short to be observed as a distinct track in a bubble chamber.

⁷C. H. Llewellyn Smith, Phys. Reports 3C, 261 (1972).

⁸T. D. Lee and C. N. Yang, Phys. Rev. 126, 2239 (1962); A. Pais, Phys. Rev. Letters 9, 117 (1962).

⁹J. D. Bjorken, Phys. Rev. 179, 1547 (1969).

¹⁰E. D. Bloom and F. J. Gilman, Phys. Rev. D 4, 2901 (1971).

¹¹F. E. Close and J. F. Gunion, Phys. Rev. D 4, 1576 (1971).

¹²The parametrization employed here is such that $F_2(\omega) \rightarrow 0$ as $\omega \rightarrow \infty$, i.e., $q^2 \rightarrow 0$ for fixed ν . On the other hand, PCAC (partially conserved axial-vector

current) relates $\nu W_2(\nu, 0)$ for the inclusive neutrino reaction to the pion-nucleon total cross section which is nonzero; e.g., see P. Langacker and M. Suzuki, Phys. Letters 40B, 561 (1972). The author has, in fact, studied the effect of parametrizing $F_2(\omega)$ such that it does not vanish as $\omega \rightarrow \infty$. The results obtained are so similar to those presented later for the parametrization of Eq. (4.2) that no additional discussion is warranted.

¹³G. Myatt and D. H. Perkins, Phys. Letters 34B, 542 (1971).

¹⁴D. Cline, A. K. Mann, and C. Rubbia, Phys. Rev. Letters 25, 1309 (1970); R. W. Brown, R. H. Hobbs, and J. Smith, Phys. Rev. D 4, 794 (1971).

A Criticism of the Accelerated-Convergence-Expansion Partial-Wave Analysis of K^+p Elastic Scattering

M. L. Griss* and G. C. Fox*

California Institute of Technology, Pasadena, California 91109

(Received 24 July 1972)

The accelerated-convergence-expansion (ACE) method of phase-shift analysis has been applied recently to K^+p elastic scattering. Its conformal-mapping technique generates larger high partial waves (HPW) than previous analyses. We calculate the HPW's from π -exchange, and estimate all possible uncertainties. The results are much smaller than and in clear contradiction with the ACE predictions for the HPW's. We suggest modifications of the latter to remedy this sad state of affairs.

I. INTRODUCTION

Recently, a new partial-wave analysis of elastic K^+p scattering has been performed¹ using the accelerated-convergence expansion (ACE) based on the method of conformal mapping and covering the range 0.5 to 2.5 GeV/c laboratory momentum.

The advantage of this method over conventional truncated Legendre expansions² is that it uses an expansion in functions more suited to the analyticity properties of the scattering amplitude; the resulting series should converge faster, making a truncated expansion in these functions need fewer terms than the conventional case. When this new series is reexpressed in terms of the usual partial waves, we discover that a "tail" of higher partial waves has been generated. In the actual ACE analysis,¹ it was possible to use fewer parameters than in the conventional analysis performed by the same group on the same data,² and the resulting solutions were more stable and with lower χ^2 .

An important and interesting test of the physical

consistency of this method is to compare the "predicted" high partial waves with the contribution to the imaginary part of the amplitude due to the major inelastic channels at these energies:

$K^+p \rightarrow K^*p$ and $K^+p \rightarrow K\Delta$.³

We find a *clear* discrepancy; the ACE high partial waves are too big by a factor which varies from about 2 to greater than 10. This is a serious criticism of the model because we estimate the uncertainty in the theoretical calculation to be at most 20%.

In Sec. II-IV, we define the theoretical models used to estimate the high partial waves. We consider the effects of π , ρ , A_2 , ω , and f^0 exchanges for the K^* and Δ reactions; also we estimate the effects of π exchange giving $I = \frac{1}{2}$ and $\frac{3}{2}$ S-wave $K\pi$ states.

In Sec. V, we confront the ACE partial waves at 1.82 GeV/c with the theoretical predictions. Given the poor agreement, we discuss in Sec. VI the theoretical uncertainties and in Sec. VII ways of modifying the ACE method to obtain agreement with our results.

II. OUTLINE OF THE CALCULATION

In this paper, we discuss two calculations of these inelastic contributions, which both find the two- π cut generated by unitarity from the single π -exchange pole; and between them we estimate corrections to this from other exchanges, and the reliability of the two- π cut itself.

In the first calculation, we use as input to the unitarity relations model amplitudes for the (quasi-) two-body processes $K^+p \rightarrow K^*p$ and $K^+p \rightarrow K\Delta$ given by Fox *et al.*⁴ These are Reggeized ρ , A_2 , ω , and f^0 exchange models; in addition, the $K^+p \rightarrow K^*p$ also includes absorbed Regge π exchange. The models give reasonable agreement with the 2.53-GeV/ c data of Brunet *et al.*⁵; most of the flexibility in the models is in the lower partial waves. However, the higher partial waves are unambiguous, dominated by π exchange in the $K^+p \rightarrow K^*p$ channel, with a lesser amount of ρ and A_2 . The partial waves are calculated by numerical integration using an extremely fine mesh (500 points).

This method is splendid for calculating the ρ - A_2 background, but it is somewhat heavy-handed, albeit correct, for the π exchange. The latter, as is well known,⁶ can be evaluated analytically by using the residue at the pole, plus the relation which for spinless scattering takes the following form:

$$\frac{1}{m_\pi^2 - t} = \frac{1}{2k^2} \sum_l (2l+1) P_l(\cos\theta) Q_l \left(1 + \frac{m_\pi^2}{2k^2} \right). \quad (1)$$

These two methods of calculating the high partial waves of K^* production agree excellently. However, in the second, we are not limited to the narrow-resonance approximation for the K^* (K - π combination), but can integrate over the contribution from all allowed K - π masses, as well as summing over the isospins and angular momenta, weighted by the appropriate K - π elastic scattering amplitude. In fact, we find that in addition to the $I = \frac{1}{2}$ P wave, there is a significant contribution to the high partial waves from the $I = \frac{1}{2}$ S wave, and a similar contribution from the $I = \frac{3}{2}$ S wave.

III. UNITARITY AND THE CONTRIBUTION OF INELASTIC CHANNELS

The formulas used in the unitarity calculation are quite simple. With $M_{\lambda\lambda'}(s, \theta)$ denoting the usual K^+p elastic amplitude, normalized so that⁷

$$\frac{d\sigma^{\text{el}}}{dt} = \frac{0.3893}{64\pi s q_i^2} \times \frac{1}{2} \sum_{\lambda\lambda'} |M_{\lambda\lambda'}(s, \theta)|^2 \text{ (mb/GeV}^2\text{)}, \quad (2)$$

we define partial waves $M_{\lambda\lambda'}^J(s)$ by

$$M_{\lambda\lambda'}(s, \theta) = 16\pi\sqrt{s} \sum_J (J + \frac{1}{2}) M_{\lambda\lambda'}^J(s) d_{\lambda\lambda'}^J(\theta). \quad (3)$$

In a similar fashion, the partial waves of the inelastic channel c , $T_{\lambda\mu\nu}^{cJ}(s)$ are related to the inelastic amplitude $T_{\lambda\mu\nu}^c(s, \theta)$ by

$$\frac{d\sigma^c}{dt} = \frac{0.3893}{64\pi s q_i^2} \times \frac{1}{2} \sum_{\lambda\mu\nu} |T_{\lambda\mu\nu}^c(s, \theta)|^2 \text{ (mb/GeV}^2\text{)}, \quad (4)$$

$$T_{\lambda\mu\nu}^c(s, \theta) = 16\pi\sqrt{s} \sum_J (J + \frac{1}{2}) T_{\lambda\mu\nu}^c(s) d_{\lambda, \mu-\nu}^J(\theta). \quad (5)$$

Unitarity relates the elastic and principal quasi-two-body channels in the following way:

$$\begin{aligned} \text{Im} M_{\lambda\lambda'}^J(s) &= q_i \sum_{\mu} M_{\lambda\mu}^J(s) M_{\lambda'\mu}^{J*}(s) \\ &+ \sum_{c, \mu, \nu} q_c T_{\lambda\mu\nu}^c(s) T_{\lambda'\mu\nu}^{c*}(s). \end{aligned} \quad (6)$$

If we now introduce the definite-parity partial waves a_ϵ^J normalized to lie within a unit unitarity circle,

$$a_\epsilon^J \equiv q_i \left(M_{\frac{1}{2}\frac{1}{2}}^J(s) + \epsilon M_{\frac{1}{2}-\frac{1}{2}}^J(s) \right) = \frac{\eta_\epsilon^J e^{2i\delta_\epsilon^J} - 1}{2i} \quad (7)$$

(ϵ is +1 or -1 and $M_{\frac{1}{2}-\frac{1}{2}}^J = M_{-\frac{1}{2}\frac{1}{2}}^J$), we obtain the final expression

$$\begin{aligned} E_\epsilon^J &\equiv \text{Im} a_\epsilon^J - |a_\epsilon^J|^2 = \frac{1 - (\eta_\epsilon^J)^2}{4} \\ &= q_i q_c \sum_{\mu, \nu} T_{\frac{1}{2}\mu\nu}^J (T_{\frac{1}{2}\mu\nu}^J + \epsilon T_{-\frac{1}{2}\mu\nu}^J)^*. \end{aligned} \quad (8)$$

Note that a_+^J has $L = J - \frac{1}{2}$ and a_-^J has $L = J + \frac{1}{2}$.

For the $K^+p \rightarrow K\Delta$ channel, we use isospin to obtain the contribution for $K^+p \rightarrow K^+\Delta^+$ from that of $K^+p \rightarrow K^0\Delta^{++}$.

In the more general case of $K^+p \rightarrow (K\pi)p$, where the $(K\pi)$ combination has isospin I , angular momentum l (spin), and helicity ν , the sum in (8) is replaced by

$$\begin{aligned} q_i \sum_{l, I} \int_{m_\pi + m_K}^{\sqrt{s} - m_p} dm \rho(m) q_c(m) \\ \times \sum_{\mu, \nu} T_{\frac{1}{2}\mu\nu}^{JI}(m) [T_{\frac{1}{2}\mu\nu}^{JI}(m) + \epsilon T_{-\frac{1}{2}\mu\nu}^{JI}(m)]^*, \end{aligned} \quad (9)$$

where $\rho(m)$ is essentially the ordinary 2-3 phase-space factor, and T^{JI} is the 2-3 amplitude, which undergoes partial-wave analysis in the s channel.⁷

It is most convenient to plot the quantity $(2J+1)E_\epsilon^J$, since this is directly proportional to

the contribution to the total inelastic cross section.

IV. DETAILS OF THE CALCULATIONS

A. Narrow-Resonance Regge Models

The model, originally fit to 5.5-GeV/ c data,⁴ is described in great detail by Fox *et al.*⁴; the amplitudes (with absorption) are evaluated numerically, using the Regge form to extrapolate to 1.82 GeV/ c . The same extrapolation describes the 2.53-GeV/ c data of Brunet *et al.*⁵ quite well.

B. Analytic Calculation of Exchange

The s -channel helicity amplitudes for the process $Kp \rightarrow (K\pi)p$ (Fig. 1) are given by

$$T_{\lambda\lambda'\nu}^{II}(\nu, \theta) = \frac{R_{\lambda\lambda'\nu}^{II}(m)}{m_{\pi}^2 - t} B_{\lambda\mu}(\cos\theta) A_{K^+\pi^0 \rightarrow (K\pi)}^{II}(m), \quad (10)$$

where R^{II} is a reduced residue at the π pole,⁸ ($t = m_{\pi}^2$), $\mu = \lambda' - \nu$, and $B_{\lambda\mu}(z)$ is the usual half-angle factor,

$$B_{\lambda\mu}(z) = \left(\frac{1+z}{2}\right)^{|\lambda+\mu|/2} \left(\frac{1-z}{2}\right)^{|\lambda-\mu|/2}. \quad (11)$$

The elastic $K\pi$ amplitude is normalized to $e^{i\delta}$, multiplied by the appropriate Clebsch-Gordan coefficient for the $K^+\pi^0$ state.

We then use the relation⁹

$$\frac{B_{\lambda\mu}(z)}{y-z} = 2 \sum (J + \frac{1}{2}) (-1)^{\lambda-\mu} e_{\lambda\mu}^J(y) B_{\lambda\mu}(y) d_{\lambda\mu}^J(z) \quad (12)$$

to obtain the partial waves (Eq. 5),

$$T_{\lambda\lambda'\nu}^{II} = \frac{R_{\lambda\lambda'\nu}^{II}}{2qq_c} A^{II} (-1)^{\lambda-\mu} B_{\lambda\mu}(y) e_{\lambda\mu}^J(y), \quad (13)$$

where

$$y = (m_{\pi}^2 + 2EE_c - 2m_p^2)/2qq_c$$

and E , E_c , q , and q_c are the center-of-mass energies and momenta of the nucleons. These are then

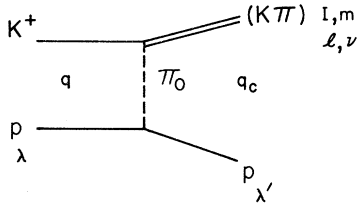


FIG. 1. One-pion exchange diagram in $K^+p \rightarrow (K\pi)p$.

inserted into Eq. (9) to get the contributions to $\text{Im}(K^+p \rightarrow K^+p)$.

We parametrize the $K\pi$ scattering amplitude for $I = \frac{1}{2}$, P wave as a Breit-Wigner resonance at the K^* :

$$A^{\frac{1}{2}1}(m) = k^3 \bar{\Gamma}_1 / [(s_{K^*} - m^2) - ik^3 \bar{\Gamma}_1] \quad (14)$$

of mass 0.89 GeV and width 0.045 GeV and roughly fit an S -wave Breit-Wigner form

$$A^{\frac{1}{2}0}(m) = k \bar{\Gamma}_0 / [(s_K - m^2) - ik \bar{\Gamma}_0] \quad (15)$$

to the "down" solution of Firestone *et al.*¹⁰ This resonance form is mainly to ensure the correct threshold behavior as $k \rightarrow 0$, and goes through 90° at $m_{K\pi} \approx 1.35$ GeV/ c^2 . (We need a rather large width = 1 GeV/ c^2 .)

For the S and P $I = \frac{3}{2}$ waves, we have used a unitarized Lovelace-Veneziano¹¹ model, which seems to give an S wave that is a little too large. The $I = \frac{3}{2}$ P wave gave a negligible contribution.

In performing the m integral, there are two important threshold effects that tend to reduce the contribution of an amplitude with respect to that in a narrow-resonance model: near $m = m_{\pi} + m_K$, $k \rightarrow 0$ and the S wave dominates, while near $m = \sqrt{s} - m_p$, $q_c \rightarrow 0$ (production threshold), so that $y \rightarrow \infty$ and the $e_{\lambda\mu}^J$ drop off rapidly with increasing J . This fact tends to make the dominant contributions come from an m value near the K^* mass. (These threshold effects also make $K^*\Delta$ production negligible.)

An effect that we observe is that the $J = \frac{1}{2}$ P -wave contribution is somewhat smaller than the narrow K^* of Sec. IV A above, but that since there is a contribution from lower values of m (corresponding to values of y closer to unity), the E_c^J do not drop off as fast with increasing J . This effect is even more pronounced for the S waves since there is only k as the threshold factor at low m , and despite the small magnitude of $(\sin\delta_0)^2$, the S wave dominates at $J \geq \frac{23}{2}$.

Although the $I = \frac{3}{2}$ S wave is smaller than the $I = \frac{1}{2}$ S wave, its contribution is increased by the Clebsch-Gordan coefficients by a factor of 2 in E_c^J . In addition, for the $I = \frac{3}{2}$, we may also include the $K^+p \rightarrow K\pi n$ channel, which gives three times as much contribution to the E_c^J as the $K^+p \rightarrow K\pi p$. This factor of 8 relative to the $I = \frac{1}{2}$ S wave makes the final contributions of the S waves about the same.

V. RESULTS

In Figs. 2(a) and 2(b), we compare the partial waves we calculate from models A and B of Sec. IV with "data" points provided by Kelly.¹² We have performed the comparison at a laboratory mo-

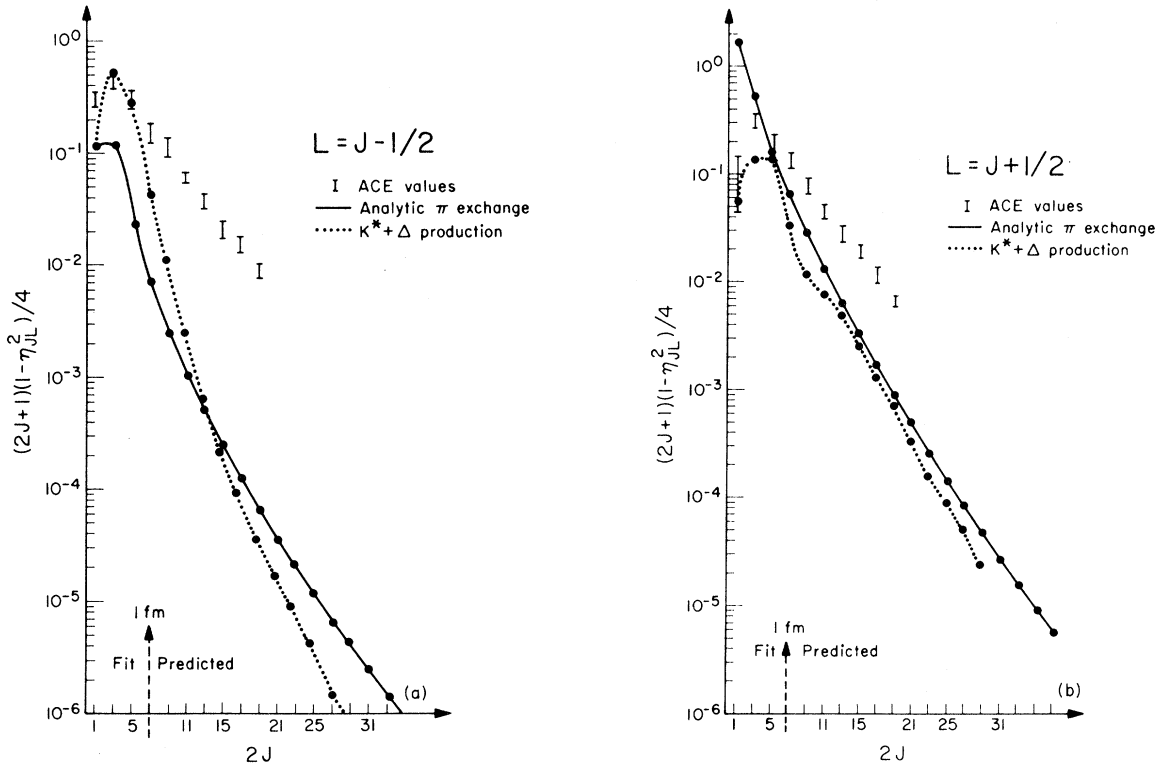


FIG. 2. Plot of the inelastic contributions $\frac{1}{4}(2J+1)(1-\eta_{JL}^2)$ for data points from Kelly (Ref. 12) at 1.82 GeV/c, analytic pion exchange (solid line), and Reggeized K^* and Δ production (dotted lines). The latter does not include the $K\pi$ S-wave contributions present in the analytic calculation. (a) Unnatural parity, $L = J - \frac{1}{2}$. (b) Natural parity, $L = J + \frac{1}{2}$.

mentum of 1.82 GeV/c, where we believe our calculation of the inelastic contributions to be most reliable. The error bars are only representative as they have been calculated for $(1-\eta_{JL}^2)$ using the $\text{Im}a_{JL}$ and $\text{Re}a_{JL}$ without considering correlations. In addition, the errors on the waves with $J > \frac{7}{2}$ have been estimated using the relative errors in the $G_{7/2}$ wave for the natural-parity sequence ($L = J + \frac{1}{2}$) and $F_{7/2}$ for the unnatural-parity sequence ($L = J - \frac{1}{2}$), as recommended by Kelly.¹² They feel that these errors are somewhat of an underestimate.¹²

It is important to notice the difference in magnitude between the $L = J + \frac{1}{2}$ sequence and $L = J - \frac{1}{2}$ sequence. Although not present in the ACE values at this energy, examination of the theoretical formulas shows that it is an unambiguous consequence of π -exchange kinematics and *must* be a feature of any theory⁸ or fit to the high partial waves. Curiously enough this size difference between the two partial-wave sequences is present in the ACE fits at other energies.

It is amusing to note that the lower waves of the absorbed Regge exchange (model A of Sec. IV),

which also includes the $K^*p \rightarrow K\Delta$ channel, are in fair agreement with the lower waves ($J \lesssim \frac{7}{2}$), which were the "free" parameters of the ACE fit; however, the higher waves disagree badly, and these are just the waves that are predicted accurately by our calculations. (One fermi is $L \sim 4$.) We conclude that the ACE method gives high partial waves that are much larger than those expected on the basis of the (dominant) physical π -exchange theory.

The relative contributions of the S and P waves and $I = \frac{3}{2}$ channel are displayed in Figs. 3(a) and 3(b).

The significance of this unusually large amount of high partial waves may be gauged from Figs. 4(a) and 4(b), where we plot the cumulative contribution of the high waves,

$$\sum_J^{\infty} (2J+1)E_\epsilon^J = \sum_J^{\infty} \frac{1}{4}(2J+1)(1-\eta_{JL}^2). \quad (16)$$

(We go "backwards" because the low waves of our models are not really realistic.) As can be seen, the tail of waves above $J \geq \frac{7}{2}$ contributes between 20% and 30% to the total inelastic cross section in the ACE method, while in our models, the higher

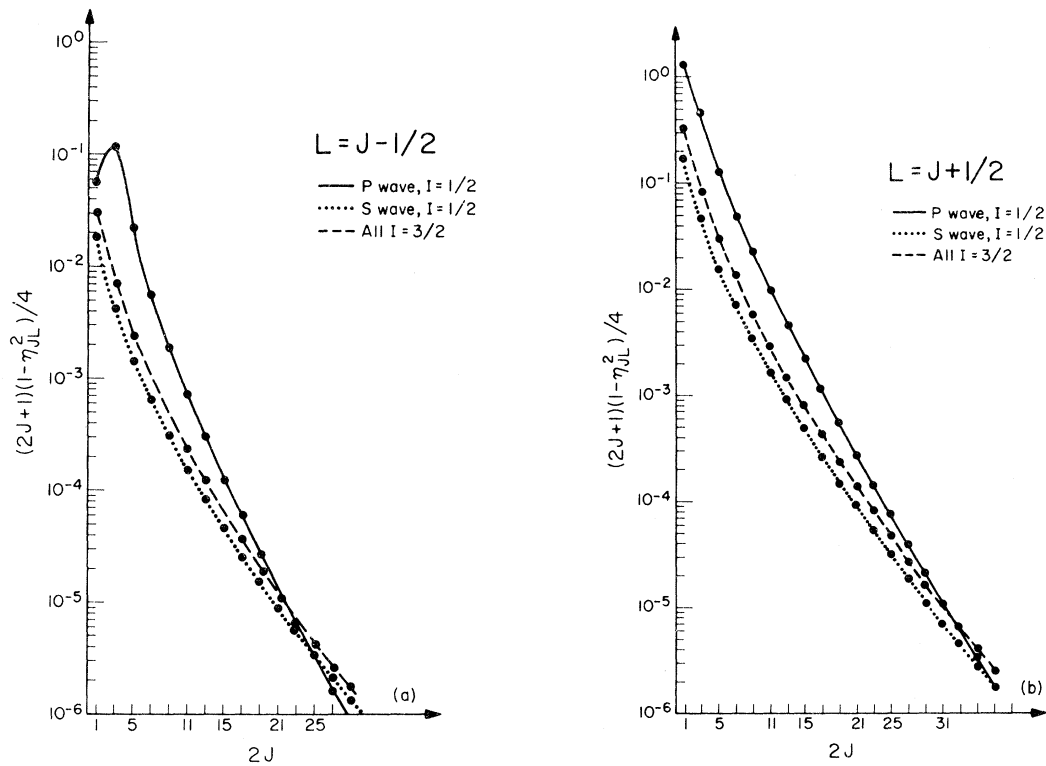


FIG. 3. Relative contributions of the $I = \frac{1}{2}$ S wave (dotted), $I = \frac{1}{2}$ P wave (solid), and $I = \frac{3}{2}$ S and P waves (dashed). (a) Unnatural parity, $L = J - \frac{1}{2}$. (b) Natural parity, $L = J + \frac{1}{2}$.

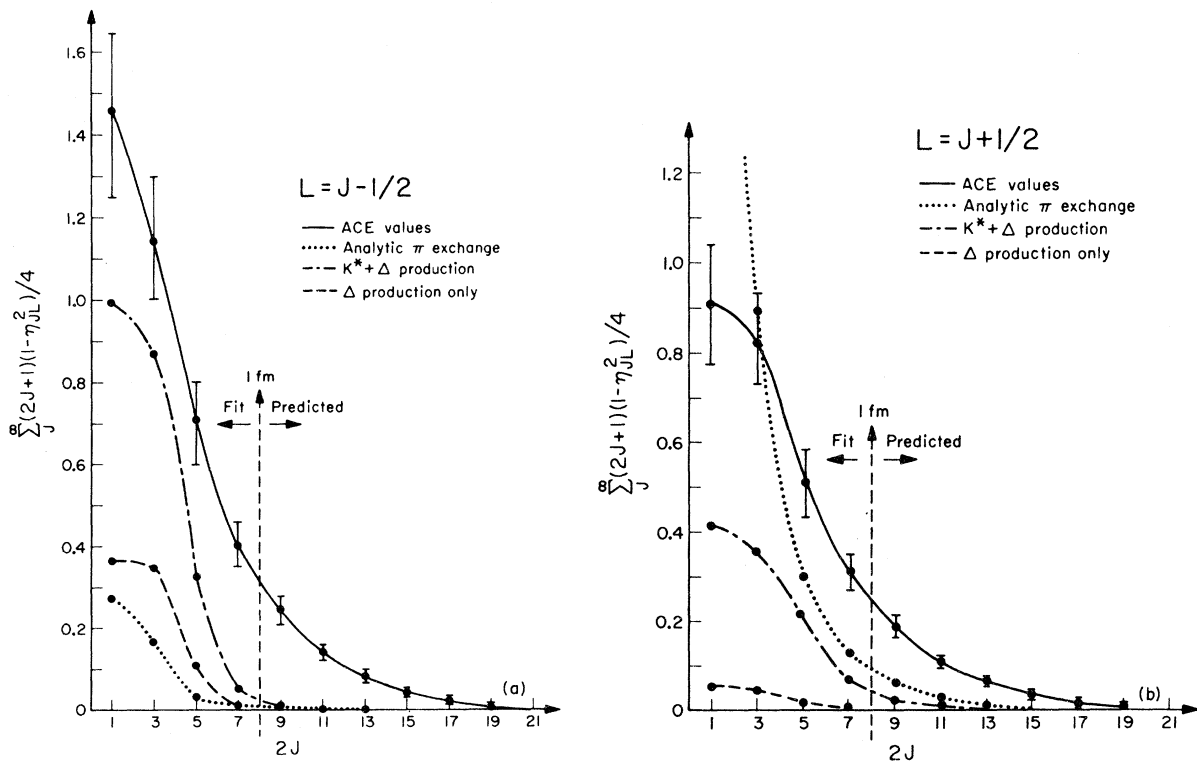


FIG. 4. Cumulative contribution of the higher partial waves to the total inelastic cross section. The waves have the same significance as in Fig. 2. (a) Unnatural parity, $L = J - \frac{1}{2}$. (b) Natural parity, $L = J + \frac{1}{2}$.

waves contribute less than $(8 \pm 2)\%$ in the $L = J + \frac{1}{2}$ sequence, and less than $(2 \pm 1)\%$ in the $L = J - \frac{1}{2}$ sequence. (The uncertainties are estimated in the next section.)

VI. UNCERTAINTIES IN THE CALCULATION

The major source of uncertainty in our values for the high partial waves is the lack of knowledge of the $K\pi$ S waves. We estimate this uncertainty to be no more than 50–60%, although the very-low-mass $K\pi$ contribution (of significance to only the highest waves, $J \geq \frac{3}{2}$) is even less well determined.

However, the S waves contribute only 10–20% to the E_c^J in the important range $J = \frac{7}{2}$ to $\frac{17}{2}$, so that the E_c^J are consequently uncertain only by 8–12% due to the S waves. Although a more realistic parametrization, including nonresonant background and constraint on the $K\pi$ scattering length could be used, the S-wave phase shifts are experimentally uncertain by at least 10–15%.

The P-wave Breit-Wigner form (K^*) is much more reasonable with the principal uncertainty of less than 5% due to the uncertainty in the K^* width. The naive k^3 barrier factor could be improved to reduce the higher- $K\pi$ -mass contributions, but this will not significantly affect our calculations.

The effect of ρ and A_2 exchange will not be included in the “analytic” π -exchange model (A of Sec. IV), but may be roughly judged from the results of model B of Sec. IV. The Δ production channel, $Kp \rightarrow K\Delta$ (essentially the two- ρ cut contribution to $K^+p \rightarrow K^+p$), is important below $J = \frac{7}{2}$, but dies away rapidly above (Fig. 4).

The only possibly important component is the interference contribution of π with the $(\rho + A_2)$ in the $Kp \rightarrow K^*p$ channel of model A (i.e., π - ρ cut). It is hard to estimate its effect in the case of broad resonances, but comparing model A with and without the ρ and A_2 contributions, we conclude that this interference affects the waves above $J = \frac{7}{2}$ by no more than a few percent. In any event, the effect is in the direction to reduce the $L = J + \frac{1}{2}$ contribution and increase the $L = J - \frac{1}{2}$ contribution;

this will certainly not spoil our conclusions.

In summary, we conservatively estimate the uncertainty on our calculated E_c^J in the range $J = \frac{7}{2}$ to $\frac{17}{2}$ to be no more than 18%.

VII. CONCLUSIONS AND DISCUSSION

There is clearly a significant discrepancy between the 20–30% contribution of the ACE high partial waves ($J > \frac{7}{2}$) and our calculation for the dominant inelastic contribution of no more than 8%.

This discrepancy arises because although the ACE method allows for a branch point in the t plane, it takes no account of the behavior of the discontinuity across the cut; in fact, this discontinuity is essentially to be determined by the ACE partial-wave analysis itself. It appears from the rate of falloff of the ACE values in Fig. 2 that ACE finds the discontinuity to be concentrated at the tip of the cut, while, in fact, the t and \sqrt{t} factors due to the large flip amplitudes, and the effect of the threshold factors in the $(K\pi)$ scattering, weaken the cut. The “effective” branch point should be considered further out.

The improved χ^2 and increased stability of the fit are probably due to the fact that ACE has inserted a tail of partial waves, giving a smooth cutoff, which suppresses the oscillations associated with the usual truncated partial-wave expansion.

We suggest two possible improvements:

(a) Repeat the analysis with more partial waves as free parameters; this will place less reliance on the ACE high partial waves. For instance, Fig. 4 indicates that the contributions of the waves above $J = \frac{13}{2}$ are less than 1% of the total. Thereby, for data of a given accuracy, one can estimate a safe cut-off point in the J plane.

(b) Use our calculated partial waves explicitly, subtracting off their contribution to the amplitude before fitting, and apply either ACE or a conventional analysis to the remainder. (In order to do this, the real parts of the high partial waves are needed and are obtained in the usual way from dispersion relations.⁶⁾)

*Work supported in part by the U. S. Atomic Energy Commission under Contract No. AT(11-1)-68 for the San Francisco Operations Office, U. S. Atomic Energy Commission.

¹R. C. Miller, T. B. Novey, A. Yokosawa, R. E. Cutkosky, H. R. Hicks, R. L. Kelly, C. C. Shih, and G. Bureson, Nucl. Phys. **B37**, 401 (1972).

²S. Kato *et al.*, Phys. Rev. Letters **24**, 615 (1970).

³The $K^+p \rightarrow K^*\Delta$ channel is suppressed by threshold effects.

⁴G. C. Fox *et al.*, Phys. Rev. D **4**, 2647 (1971); D. Johnson *et al.*, Argonne report, 1972 (unpublished).

⁵J. M. Brunet *et al.*, Nucl. Phys. **B37**, 114 (1972).

⁶J. W. Allcock and W. N. Cottingham, Nucl. Phys.

B31, 443 (1971).

⁷H. Pilkuhn, *Interactions of Hadrons* (North-Holland, Amsterdam, 1967).

⁸This comes from the normal π contribution to the $2 \rightarrow 3$ process, $KN \rightarrow K\pi N$, with the helicities crossed to the s channel. For further details, see *Proceedings of the Conference on $\pi\pi$ and $K\pi$ Interactions, Argonne National Laboratory, 1969*, edited by F. Loeffler and E. D. Malamud (Argonne National Laboratory, Argonne, Ill., 1969).

⁹P. D. B. Collins and E. J. Squires, in *Springer Tracts in Modern Physics*, edited by G. Höhler (Springer, New York, 1968), Vol. 45.

¹⁰A. Firestone *et al.*, Phys. Rev. D **5**, 2188 (1972).

¹¹C. Lovelace, invited paper, in *Proceedings of the Conference on $\pi\pi$ and $K\pi$ Interactions, Argonne National Laboratory, 1969* (Ref. 8).

¹²R. L. Kelly (private communication). These values are preliminary results of additional work beyond that reported in Ref. 1.

PHYSICAL REVIEW D

VOLUME 7, NUMBER 1

1 JANUARY 1973

Proton Distributions in High-Energy Proton-Proton Collisions*

Richard Slansky

Physics Department, Yale University, New Haven, Connecticut 06520

(Received 3 August 1972)

The spectrum of protons in proton-proton collisions is analyzed in terms of a fragmentation model. Particular attention is devoted to the strength of the isobar production and the energy dependence of the background. The model reproduces the shape and energy dependence of the proton spectrum in a very detailed way. Some problems of identifying production mechanisms from these data are discussed.

I. INTRODUCTION

The spectrum of fast protons in proton-proton collisions is an important source of information about nucleon isobars and production mechanisms. Some of these fast protons are quasielastic protons in channels of the type

$$p + p \rightarrow p + N^* . \quad (1)$$

The most transparent cross section for studying these channels is $d^2\sigma/dMdt$, where M is the missing mass of the observed proton (the N^* mass), and $-t$ is the square of the momentum transfer to the observed proton. If other processes could be eliminated, $d^2\sigma/dMdt$ would be just the cross section for isobar (N^*) production. However, it is not easy to extract this cross section, because there is an energy-dependent "background" of protons from other processes, as seen in Fig. 1.¹ One source of background protons comes from the decay of isobars produced in single- and double-excitation processes. These fragmentation protons may be detected at low missing masses if the incident proton energy is not too high. They are most simply studied in terms of the invariant distribution

$$f(x, k_T^2, s) = \frac{2\omega_k}{\pi\sqrt{s}} \frac{d^2\sigma}{dx dk_T^2} , \quad (2)$$

where $x = 2k_L/\sqrt{s}$, and k_L , k_T , and ω_k are respectively the longitudinal momentum, transverse momentum, and energy of the observed proton in the reaction center-of-mass system. The invariant distribution of fragmentation protons is expected to scale, which implies an energy-dependent contribution to $d^2\sigma/dMdt$. Of course, other contributions to the background may also be present.

The separation of quasielastic and background protons has not been carried out in a model-independent manner. For want of a better method, the isobar cross section is often estimated by drawing a smooth background curve just below the resonance peaks.^{1,2} Evaluated in this way, the cross section for exciting the target into an isobar with a mass less than 2 GeV is only about 1 mb. This leaves a large background of protons. Since the behavior of the background is expected to reflect some information about production mechanisms, it has been the subject of considerable discussion. One would hope that the available data, which cover a wide range of energies and momentum transfers,¹⁻⁷ should provide some check on the proposed mechanisms. Even so, the data appear to be compatible with several points of view. Perhaps the most popular framework used to study this problem is the triple-Regge formalism.⁸ This model is appropriate for large missing mass, M , and large $\sqrt{s} \gg M$. Among other things, it is